A decision support system for the development of voyage and maintenance plans for ships

Abstract

The waterborne sector faces nowadays significant challenges due to several environmental, financial and other concerns. Such challenges may be addressed, among others, by optimising voyage plans, and diagnosing as early as possible engine failures that may lead to performance degradation. These two issues are addressed by the Decision Support System (DSS) presented herein, which focuses on the operation of merchant ships. For the development of voyage plans, a multicriteria decision problem is developed and handled with the PROMETHE method, while a multivariable control chart is used for the fault diagnosis problem. A MATLAB-based software implementation of the DSS has been developed adopting a modular architecture, while, in order to provide a generic software solution, the required input data are retrieved from dedicated web-services, following specific communication and data exchange protocols.

Keywords

Voyage plan, marine engine fault diagnosis, condition based maintenance, decision support systems, multicriteria decision analysis

1. Introduction

Environmental concerns in light of climate change, societal pressure for cleaner transport modes, competition, rising oil prices, potential oil shortages in the long term, and increased traffic congestion are some only of the many challenges that the waterborne transport sector needs to address nowadays (EC, 2011). For their part, owners and operators are interested in their ship competitiveness once they are operating, which may be achieved by improving the energy efficiency of vessels, optimising voyage plans, or through the development of innovative vessels based on designs and construction techniques, which reduce operation and maintenance costs (EC, 2011).

From the operational point of view, the new practice of slow steaming i.e. sailing at lower speed can reduce fuel consumption and as result, the relevant costs and the resulting pollutant emissions. If a ship that normally sails at 18 knots slows down to 14 knots, it can reduce the gaseous emissions by 40%, a difference that is due to the fact that the propulsion power varies with ship speed in a power of 3 or more (EC, 2011). However, the ship speed is strongly related to the load condition, sea states, currents and winds, as well as any existing constraints on Estimated Time of Arrival (ETA), factors that although should be well considered and balanced while developing a voyage plan, cannot be easily taken into account in the maximum possible extend while manually developing voyage plans. In addition, appropriate and timely ship maintenance is a prerequisite to preserve the engine at an operating level that would allow slow steaming produce real benefits. The Decision Support System (DSS) presented in this paper is built upon these two pillars i.e. the development of voyage plans considering factors such as the ones mentioned above, and the early diagnosis of engine failures that would allow a timely planning of maintenance activities.

In contrast to other approaches presented in the relevant literature (see Psaraftis and Kontovas (2012) for a comprehensive review), which mainly focus on the operations of ship fleets when criteria such as cost effectiveness and environmental friendliness are considered, the approach followed by the DSS presented herein, focuses on the operation of merchant ships. A similar focus is also present in other proposed methods and corresponding DSS, which take into account environmental data, ship responses and hull condition. For example, a new weather-routing algorithm based on the composite influence of multi-dynamic elements for determining the optimised ship routes has been recently proposed by Lin et al. (2013). Also, Kosmas and Vlachos (2012) developed a simulated annealing based algorithm for the determination of optimal ship routes through the minimisation of a cost function including effects of voyage time and comfort, as well as safety factors. Furthermore, various expert systems have been developed to aid shipboard personnel for solving ship main and auxiliary machinery troubleshooting (Cebi et al., 2012). Unlike these approaches, however, the problem of developing voyage plans is not addressed by the DSS proposed herein via a rigorous mathematical optimisation procedure (Psaraftis and Kontovas, 2012), but rather faced as a mutlicriteria decision one, thus multicriteria decision aid (MCDA) techniques are employed to model and solve it.

MCDA (Figueira et al, 2005) is a scientific discipline that includes several approaches, models and methods aiming at handling and evaluating problems where multiple criteria have to be taken into account. The main difference and advantage of MCDA compared to other alternative approaches is that is does not simply synthesises all the problem parameters, synthesis that may be achieved equally well by other approaches, such as e.g. mathematical optimisation, but is makes this synthesis in the light of the decision making policy, as well as the preferences, priorities and value system that the corresponding decision maker (DM), consciously or unconsciously, uses.

The rest of the paper is structured in four more sections. Section 2 provides an overview of the overall DSS, while Sections 3 and 4 describe its main modules and software implementation, respectively. Section 5, finally provides some concluding remarks along with suggested future extensions of the system.

2. DSS Overview

As mentioned earlier, the aim of the DSS presented herein is to support and contribute to the cost effective and environmental friendly operation of ships via the development of appropriate voyage plans and the diagnosis of engine failures in order to develop timely maintenance plans. Figure 1 provides an overview of the DSS.

< insert figure 1 >

As far as the voyage plans are concerned, upon a user request, the DSS is fed with data concerning the departure and arrival ports, and the main route connecting them, as well as the particular ship that will undertake the trip and its load condition, a range of acceptable mean speeds as well as any existing constraints on fuel consumption, emitted pollutants and arrival time. In addition to these user-provided data, the DSS retrieves data regarding the prevailing sea states, currents and winds around the main route from internet-based weather services (see Section 4.4 below for external data acquisition). Using these data, it develops and displays to

the user several alternative voyage plans ordered according to the preferences that he/she has expressed to criteria such as fuel consumption, pollutant emissions and travel time.

In the heart of the corresponding DSS module that is responsible for the development of the voyage plans, the PROMETHE (Preference Ranking Organisation Method for Enrichment Evaluation) II methodology lies, which allows for the complete ranking of the considered alternative voyage plans. The same module includes also a ship propulsion system model, which evaluates each developed voyage plan against the criteria of concern to the user. Section 3.1 below provides an insight to this DSS module and the adopted MCDA approach. PROMETHE II has been selected for this DSS for its simplicity, which is a significant element for this particular application that is addressed to DMs that do not necessarily possess the knowledge required for the application of other more advanced MCDA methods, as well as for its non-compensatory nature that prevents alternatives to be selected, which may outperform in some criteria but have a really low performance in others.

As far as the detection of the ship's engine failure is concerned, a multivariable control chart based on the Mahalanobis distance is used. In this way, the interrelation of the various measured variables is taken into account (Bersimis et al., 2005). A systematic analysis of cause-effect relations amongst the various monitored parameters and the most common marine engine faults, reveals the necessary sensors that need to be employed. Extensive simulations on normal engine operation provide the no-fault statistics, while selective fault conditions verify the effectiveness of the proposed algorithm. The whole plan is further tested with near-real life conditions, utilising an experimental laboratory engine and the system's remote data acquisition system.

The particular DSS module implementing the fault diagnostics runs at discrete user-specified time intervals. An insight to this module is provided in Section 3.2.

The software implementation of the DSS platform has been based in MATLAB. Here, a modular architecture has been adopted, where the voyage plan development and the fault detection functionalities are developed as different modules, accompanied by separate Graphical User Interfaces (GUIs). In the former module, separate panels for the trip data, the ship data and the user preferences have been defined, while these data are used as inputs to the model of the ship and the PROMETHE II method, in order to evaluate the best alternative voyage plan. In the latter module, a pre-defined set of engine parameters measurements is provided and the fault detection function estimates if an engine fault is present. Here, the notification on a possible fault is accompanied by some statistical information on the values of the monitored engine parameters, in order to provide additional information to the maintenance staff for determining the root cause of the problem.

In an effort to provide a generic software solution, the input data required by the DSS platform are retrieved from dedicated web-services, following specific communication and data exchange protocols. Section 4 below provides an insight to the software implementation and the interfaces of the DSS.

3. DSS modules

3.1. Voyage plan development module

3.1.1. Methods and tools

Within this DSS module, the development of a voyage plan is formulated as a mutlicriteria decision problem whereby several alternative plans are developed, evaluated against different decision criteria and ranked from the most to the least satisfactory plan according to the preferences and priorities of the user. As mentioned earlier, for the ranking of the alternative plans the PROMETHE II method is adopted.

PROMETHE II (Brans and Mareschal, 2005; Moffett and Sarkar, 2006; San Cristóbal Mateo, 2012) is one of the most widely used methods of the family of outranking MCDA, a scientific discipline that includes several approaches, models and methods aiming at handling and evaluating problems where multiple criteria have to be taken into account for the evaluation of alternative actions. Based on the principle of their pairwise comparison, PROMETHE II provides a full ranking of all the examined alternative actions. This ranking provides the best compromise solutions according to the evaluation criteria, the preferences and the priorities of the decision maker (DM).

To apply PROMETHE II, one has to define the set of alternative actions to be ranked, the set of criteria to be used for the ranking, as well as weights reflecting the preferences and priorities of the DM with respect to the criteria. Based on these, a multicriteria table is created, which includes the evaluation of each alternative action against each considered criterion. In addition, a preference function is defined for each criterion that reflects the preference of an action from another according to this criterion.

In the PROMETHE II method, the following six preference functions represented by specific shapes are available for the pairwise comparison of the alternative actions (Brans and Mareschal, 2005; Moffett and Sarkar, 2006; San Cristóbal Mateo, 2012):

- Usual criterion (type 1)

$$P_n\left(A_i, A_j\right) = \begin{cases} 0, \text{ αν } g_n\left(A_i\right) - g_n\left(A_j\right) \le 0 \\ 1, \text{ αν } g_n\left(A_i\right) - g_n\left(A_j\right) > 0 \end{cases}$$

- U-shape criterion (type 2)

$$P_n\left(A_i, A_j\right) = \begin{cases} 0, \text{ αν } g_n\left(A_i\right) - g_n\left(A_j\right) \le q_n \\ 1, \text{ αν } g_n\left(A_i\right) - g_n\left(A_j\right) > q_n \end{cases}$$

- V-shape criterion (type 3)

$$P_n\left(A_i, A_j\right) = \begin{cases} 0, & \text{αν } g_n\left(A_i\right) - g_n\left(A_j\right) \le 0 \\ \dfrac{g_n\left(A_i\right) - g_n\left(A_j\right)}{p_n}, & \text{αν } 0 \le g_n\left(A_i\right) - g_n\left(A_j\right) \le p_n \\ 1, & \text{αν } g_n\left(A_i\right) - g_n\left(A_j\right) > p_n \end{cases}$$

- Level criterion (type 4)

$$P_n\left(A_i, A_j\right) = \begin{cases} 0, & \text{αν } g_n\left(A_i\right) - g_n\left(A_j\right) \le q_n \\ 1/2, & \text{αν } q_n < g_n\left(A_i\right) - g_n\left(A_j\right) \le p_n \\ 1, & \text{αν } g_n\left(A_i\right) - g_n\left(A_j\right) > p_n \end{cases}$$

- V-shape with indifference criterion (type 5)

$$P_n\left(A_i, A_j\right) = \begin{cases} 0, & \alpha\nu\ g_n\left(A_i\right) - g_n\left(A_j\right) \le q_n \\ \dfrac{g_n\left(A_i\right) - g_n\left(A_j\right) - q_n}{p_n - q_n}, & \alpha\nu\ q_n < g_n\left(A_i\right) - g_n\left(A_j\right) \le p_n \\ 1, & \alpha\nu\ g_n\left(A_i\right) - g_n\left(A_j\right) > p_n \end{cases}$$

- Gaussian criterion (type 6)

$$P_n\left(A_i, A_j\right) = \begin{cases} 0, & \alpha\nu\ g_n\left(A_i\right) - g_n\left(A_j\right) \le 0 \\ 1 - e^{-\frac{\left(g_n(A_i) - g_n(A_j)\right)^2}{2(s_n)^2}}, & \alpha\nu\ g_n\left(A_i\right) - g_n\left(A_j\right) > 0 \end{cases}$$

where, $P_n(A_i, A_j)$ is the preference of an alternative A_i over an alternative A_j for a given criterion n, $g_n(A_i)$ and $g_n(A_j)$ are the evaluations of alternatives A_i and A_j for the considered criterion, and q_n, p_n and s_n are thresholds that define the shape of the corresponding preference functions. More specifically, q_n is an indifference threshold representing the largest difference of the evaluations $g_n(A_i)$ and $g_n(A_j)$ of two alternative actions that is considered negligible, p_n is a preference threshold representing the smallest difference that is considered as decisive, and s_n is a threshold in between q_n and p_n that defines the inflection point of the corresponding preference function.

The selection of an appropriate function as well as the definition of its parameters requires generally a good knowledge of the methodological approach of PROMETHE II as well as of the implications that such choices have on the results. In case that such knowledge is not available and/or desirable, as in the case of the DM which will be the user of the DSS proposed herein, i.e. the ship owner and/or operator, the Gaussian type preference function (i.e. the function type 6) should be better selected. This particular function possesses two distinguished properties compared to the others:

- To define the Gaussian criterion function type for a particular criterion n, only the inflection point represented by threshold s_n needs to be defined. This threshold is typically computed via the standard deviation of the evaluations of the alternative actions against the considered criterion.
- It is the only function type that does not have discontinuities. It may therefore ensure stability of the results. Stability is of great importance since it concerns the magnitude at which the values of the involved parameters affect the results. Since the DM is not always capable to define accurate values for the involved parameters, it is important for the results to be stable, i.e. to not present significant variance when small deviations are introduced to the parameter values. On the other hand of course, it is necessary for the results to vary significantly for large deviations of the parameter values. Otherwise, the method has failed in taking into account the particularities of each different case.

Based on the selected preference functions, an aggregated preference index $\pi(A_i, A_j)$ is then calculated for each pair of alternative actions A_i, A_j as follows

$$\pi\left(A_i, A_j\right) = \sum_{n=1}^{N} W_n P_n\left(A_i, A_j\right)$$

with N the total number of considered criteria and W_n the weight of each criterion n according to the involved DM. The aggregated preference index expresses the overall preference of the one alternative over the other, and is used to develop for each alternative action two further indices:

- The positive outranking flow $\varphi^+(A_i) = \sum_{A_j} \pi(A_i, A_j) \big/ n-1$, which expresses the degree to which an action A_i is preferred over all the other alternatives A_j; and
- The negative outranking flow $\varphi^-(A_i) = \sum_{A_j} \pi(A_j, A_i) \big/ n-1$, which expresses the degree to which all the other actions A_j are preferred from this specific one.

The difference $\varphi^+(A_i) - \varphi^-(A_i)$ of the aforementioned two flows is the net outranking flow $\varphi(A_i)$, which reflects the overall preference, of the corresponding DM, for the alternative action A_i, and is used to rank the alternatives in such a way that the larger the net flow of an alternative, thus its preference by the DM, the higher its rank order relative to the other ones.

3.1.2. Applying PROMETHE II to the voyage plan development problem

To apply the PROMETHE II method to the problem at hand, the alternative voyage plans i.e. the alternative actions to be ranked, need to be developed at first. These plans are generated by a combination of the available alternative solutions regarding the route, the speed, and the fuel type. To this end, the main route connecting the departure and arrival ports is first designated by the user. This route is divided in three main segments for each of which the user defines acceptable speeds and fuel types. These three segments practically correspond to the three main parts of a trip: departure, cruising, arrival. The designated main route is then used to define a corridor within which several alternative routes can be developed. The alternative routes in combination with the acceptable speeds and fuel types defined by the user for each part of the main route are finally used to determine the set A of the alternative voyage plans that will be examined and ranked. Therefore, each alternative voyage plan $A_m \in A$ with $m = 1, \ldots, M$ the plan index and M the total number of defined plans comprises of a specific route from the departure to the arrival port, with a given speed and fuel type for each of its three main parts. Obviously, the aforementioned process may lead to an extremely large set A of alternative voyage plans the examination of which would have been practically impossible without the assistance of a DSS.

The alternative voyage plans developed through the previously described procedure are then evaluated in terms of criteria that reflect the cost effective and environment friendly aims set forth for the ship operation. The set C of criteria C_n with $n = 1, \ldots, N$ the criterion index and N the total number of criteria, adopted by the DSS in this respect includes:

- The volume of consumed fuels, a criterion that reflects the operational cost which should be minimised;
- The travel time, a criterion that reflects the ETA, and it should also be minimised;
- The volumes of released CO_2 and SO_2 emissions, criteria that reflect the trip's environmental impacts, and need also be minimised.

User-defined constraints on these criteria may also be defined, as necessary, to eliminate from the set of alternatives to be ranked by PROMETHE II, those that are a priori known to not satisfy given needs and limitations of the DM (e.g. given budget and/or time constraints).

Given the above, it is obvious, that it is not possible to identify even a single voyage plan $A_m \in A$ that could satisfy, i.e. minimise all the above criteria simultaneously. A voyage plan, for example, incorporating higher speeds would minimise the travel time, to the detriment, however, of all the remaining criteria. A plan on the other hand incorporating lower speeds would increase the travel time but would decrease the fuels' volume and the corresponding released emissions. Finally, depending on the particular fuels utilised, different volumes of CO_2 and SO_2 emissions would be released in the environment for the same speed levels. Consequently, all the considered criteria are necessary for the DM to develop in a cost effective and environmental friendly way voyage plans, which will also allow the ship to reach its destination the sooner possible or, at least, satisfying, as much as possible, any potential ETA-related requirements and constraints. Beyond their necessity, these criteria are also competitive and they incorporate a trade-off that should be carefully balanced by the DM according to his/her preferences and priorities, which are expressed via the respective criteria weights W_n with $n = 1, \ldots, N$.

To evaluate each alternative voyage plan against each considered criterion, i.e. to develop the multicriteria table, a ship model is required. Such model, taking into account the characteristics of each alternative plan, i.e. the route, the speed and fuel type at each route segment as well as the sea states, currents and winds, will estimate the required volume of fuels, the corresponding volumes of CO_2 and SO_2 emissions that will be released, and the time that will be required for the ship to reach its destination under this plan. Plans that do not satisfy potentially existing user-defined constraints on these criteria are excluded so that the final decision problem formulation necessary for the application of PROMETHE II is reached.

In this particular DSS version, a ship model developed based on a specific ship propulsion system type has been used. It is possible, however, to develop, import in the DSS and use other ship models too, depending on the specific requirements of a particular trip.

3.2. Fault diagnosis module

3.2.1. Engine fault simulator

Marine engine fault diagnosis has been investigated by many authors (Kyrtatos, 1989; Hountalas, 2000; Benvenuto and Campora, 2007; Lamaris and Hountalas, 2010). However, it remains a difficult problem due to the complexity of the engine system, and the variation of the external influences. In this study, the ship main engine is regarded as a disturbance attenuation PID controlled system (Figure 2).

<insert figure 2 >

The ship main engine, which is of the two-stroke marine Diesel type for the majority of merchant ships, is modelled using a modular concept by interconnecting flow receiver elements (control volumes) with flow elements. Fixed fluid elements with constant pressure and temperature are used for modelling the engine boundaries. Shaft elements are used for calculating the engine crankshaft and turbocharger shaft rotational speeds by solving the differential equations which are derived by applying the angular momentum conservations. The propeller torque is calculated considering the propeller law, whereas the engine fuel rack position is provided as input. The model was also implemented in the MATLAB/Simulink environment as shown in Figure 3. Thus, the modelled engine elements form discrete

subsystems, which exchange the required variables through appropriate connections. The flow elements use as input the pressure, temperature and the properties of the working medium (air or gas) contained in the adjacent elements (flow receiver(s) or fixed fluid), whereas their output includes the mass flow and energy rates entering and exiting the flow element as well as the absorbed (for the case of compressor) or produced torques. The former are provided as input in the adjacent flow receiver elements, whereas the latter is required as input in the shaft elements. The output of shaft elements, i.e. the engine crankshaft and turbocharger shaft rotational speeds, are supplied as input to the respective flow controller. The detailed description of the used model can be found in Theotokatos (2010), while below its main elements are outlined (see Table 1 for list of adopted model symbols).

< insert figure 3 >

< insert table 1 >

The flow receiver elements are modelled using the open thermodynamic system concept (Watson and Janota, 1982). The working medium mass and temperature are calculated using the following differential equations, which are derived by applying the mass and energy conservation laws in each volume, respectively:

$$\frac{dm}{dt} = \dot{m}_{in} - \dot{m}_{out}$$

$$\frac{dT}{dt} = \frac{\dot{Q}_{ht} + (\dot{m}h)_{in} - (\dot{m}h)_{out} - u\frac{dm}{dt}}{mc_v}$$

where $\dot{m}_{in}$, $(\dot{m}h)_{in}$ are the mass flow and energy rates entering the flow receiver, and $\dot{m}_{out}$, $(\dot{m}h)_{out}$ are the mass flow and energy rates exiting the flow receiver, respectively. Subsequently, the working medium pressure is calculated using the ideal gas law.

No heat transfer is taken into account for the scavenging air receiver, whereas the transferred heat from the gas contained in the exhaust gas receiver to the ambient is calculated using the exhaust gas receiver overall heat transfer coefficient and heat transfer area. The overall heat transfer coefficient in the exhaust receiver is calculated using a Nusselt-Reynolds number correlation for gas flowing in pipes (Rohsenow et al., 1985).

The engine cylinders bank is regarded as a flow element, where the incoming air mass flow rate is calculated considering the equivalent of two consecutive orifices, each one representing the cylinders scavenging ports and exhaust valve, respectively (Meier, 1981). Thus, the engine cylinders air mass flow rate is calculated based on subsonic flow consideration (Heywood, 1988) using the equivalent cylinders flow area, the air properties and the pressures upstream and downstream of the engine cylinders. The equivalent orifice geometric area can be estimated using the instantaneous area variations for an engine cycle of the intake ports and exhaust valves, as proposed in Meier (1981).

The mass flow rate of the exhaust gas exiting the engine cylinders is found by adding the mass flow rates of the air entering the engine cylinders and the injected fuel. The latter is calculated using the number of the engine cylinders, the engine rotational speed and the injected fuel mass per cylinder and per cycle. The injected fuel mass per cylinder and per

cycle is regarded as function of engine fuel rack position.

The energy flow rate exiting the engine cylinders element is calculated by taking into consideration the energy conservation equation and the fact that a portion of the fuel energy remains in the exhaust gas; thus:

$$(\dot{m}h)_{cyl\_d} = \dot{m}_a h_{a\_cyl\_u} + \zeta \eta_{comb} \dot{m}_f H_L$$

where ζ is fuel chemical energy proportion in the exhaust gas exiting engine cylinders.

The proportion of the fuel chemical energy contained in the exhaust gas is considered to be a function of the engine brake mean effective pressure (Meier, 1981), which is calculated using available engine performance data measured during the engine trials or provided by the engine manufacturer. The indicated mean effective pressure is calculated using the rack position, the maximum indicated mean effective pressure of the engine and the combustion efficiency, which, in turn, is regarded as function of engine air to fuel ratio (Watson and Janota, 1982). The friction mean effective pressure is considered function of the indicated mean effective pressure and the engine crankshaft speed. The engine brake mean effective pressure is calculated by subtracting the friction mean effective pressure from the indicated mean effective pressure, whereas the engine torque is calculated using the brake mean effective pressure and engine cylinders displacement volume (Heywood, 1988).

The compressor is modelled using its steady state performance map, which is provided as input in a digitised form containing lines of the turbocharger speed, pressure ratio, corrected flow rate and efficiency. Given the turbocharger shaft speed and the compressor pressure ratio, the corrected flow rate and efficiency are calculated using interpolation. The turbocharger shaft speed is taken from the turbocharger shaft element, whereas the compressor pressure ratio is calculated by the following equation using the pressure of the fixed fluid connected upstream the compressor, the pressure of the scavenging air receiver connected downstream the compressor, the air filter pressure drop, the air cooler pressure drop and the pressure increase in the auxiliary blower:

$$pr_C = \frac{p_{SC} - \Delta p_{AC} + \Delta p_{BL}}{p_{amb} - \Delta p_{AF}}$$

The air filter and air cooler pressure drops are considered to be proportional to the compressor air mass flow rate squared, whereas the blower pressure increase is regarded as function of its volumetric flow rate. The temperature of the air exiting compressor is calculated based on the compressor isentropic efficiency definition equation (Watson and Janota, 1982) using the temperature of the air entering the compressor and the compressor pressure ratio and efficiency.

The temperature of the air exiting the air cooler is calculated based on the air cooler effectiveness definition equation (Watson & Janota, 1982) using the air cooler effectiveness and the temperature of the cooling water entering the air cooler. The air cooler effectiveness is assumed to be a polynomial function of the air mass flow rate. The compressor absorbed torque is calculated by the following equation:

$$Q_C = 30\dot{m}_C \left(h_{C\_d} - h_{C\_u} \right) / (\pi N_{TC})$$

where the enthalpies of the air exiting the compressor and the air entering the compressor are calculated using the respective temperatures.

The turbine is modelled using its swallowing capacity and efficiency maps, which must be provided in digitised form. Given the turbine pressure ratio, the turbine mass flow rate and efficiency are calculated using interpolation. The turbine pressure ratio is calculated using the pressure of the exhaust gas receiver, the ambient pressure downstream the engine exhaust pipe and the exhaust pipe pressure loss, as follows:

$$pr_T = \frac{p_{ER}}{p_{amb} + \Delta p_{ep}}$$

The pressure loss of the exhaust piping system is regarded as proportional to the exhaust gas mass flow rate squared. The temperature of the gas exiting turbine is calculated based on the turbine isentropic efficiency definition equation (Watson and Janota, 1982) using the temperature of gas entering turbine, and the turbine pressure ratio and efficiency. The turbine torque provided to the turbocharger shaft is derived by using the following equation:

$$Q_T = 30\dot{m}_T \left(h_{ER} - h_{T,d} \right) / (\pi N_{TC})$$

where the enthalpy of the gas exiting the turbine is calculated using the respective temperature, whereas the enthalpy of the gas entering the turbine is taken from the upstream exhaust gas receiver element.

The engine crankshaft and turbocharger shaft rotational speed calculation is carried out in the shafting system and turbocharger shaft elements, respectively. The former uses the engine and propeller torques fed from the engine cylinders and propeller elements, respectively; the later uses the compressor and turbine torques supplied form the respective elements. The propeller torque is calculated by applying the propeller law equation passing through the engine maximum continuous rating (MCR) point.

The engine crankshaft and turbocharger shaft rotational speeds are calculated by integrating the following equations derived using the angular momentum conservation in the propulsion plant shafting system and the turbocharger shaft, respectively:

$$\frac{dN_E}{dt} = \frac{30\left(\eta_{Sh} Q_E - Q_P\right)}{\pi\left(I_E + I_{Sh} + I_P + I_{ew}\right)}$$

$$\frac{dN_{TC}}{dt} = \frac{30\left(Q_T - Q_C\right)}{\pi I_{TC}}$$

In order to make a starting list of the targeted fault conditions, the most frequent engine fault cases were considered as derived by Kawasaki (1980) and Banisoleiman and Rattenbury (2006) (see Figure 4). Furthermore, taking into account the limitations of the employed engine simulator, the targeted fault list is formed as in Table 2, while, in order to construct a fault cause-effect table, the Simulink diagram of Figure 5 is used.

< insert figure 4 >

< insert table 2 >

< insert figure 5 >

After an excessive number of simulation runs, we arrived at Table 3. This table was constructed by noting the most significant effect each fault had on the system's variables. Faults were simulated by changing appropriate parameters of the ship's engine model.

<insert table 3 >

3.2.2. Engine fault detection procedure and results

The fault diagnosis subsystem is based on a multivariable Shewart control chart structure (Mason, 2002), an approach mainly used for fault detection. Fault isolation is also possible, however not pursued in this study. In order to implement the fault diagnosis subsystem:

- No fault (healthy) data is collected, in order to estimate the healthy operation statistics (to be used in the fault detection algorithm). A representative sample was created using the values of Table 4. Thus, a total of 7986 samples were collected;

< insert table 3 >

- The sample mean vector $\hat{m}$ and sample covariance matrix $\hat{\Sigma}$ of the healthy data set X are calculated using the usual unbiased estimates,

$$X = \begin{bmatrix} Twac(1) & Ta(1) & FR(1) & s_1(1) & \cdots & s_{12}(1) \\ Twac(2) & Ta(2) & FR(2) & s_1(2) & \cdots & s_{12}(2) \\ \vdots & \vdots & \vdots & \vdots & \ddots & \vdots \\ Twac(7986) & Ta(7986) & FR(7986) & s_1(7986) & & s_{12}(7986) \end{bmatrix}$$

$$\hat{m} = \frac{1}{N}\sum_{i=1}^{N} x_i, \quad \hat{\Sigma} = \frac{1}{N-1}\sum_{i=1}^{N}(x_i - \hat{m})(x_i - \hat{m})^{\mathrm{T}}$$

- The control chart UCL (upper control limit) is calculated, using the fact that the Mahalanobis distance,

  $D_m = \sqrt{(x - \hat{m})\hat{\Sigma}^{-1}(\hat{x} - \hat{m})^{\mathrm{T}}}$

  follows the χ^2 distribution with n degrees of freedom. Therefore, at significance level a = 0.95, UCL = χ^2(0.99, 15) = 30.58.

In order to test the proposed algorithm, each fault from Table 3 was simulated using a random value from Table 4. All faults were satisfactorily detected.

As an example, the control chart for a simulated fault in the air cooler is shown in Figure 6. Air cooler fouling results in the reduction of air cooler effectiveness ε_{AC}, which is calculated as a function of air cooler mass flow rate $\dot{m}_a$ using the following equation:

$$\varepsilon_{AC} = k_{AC0} + k_{AC1}\,\dot{m}_a + k_{AC2}\,\dot{m}_a^2$$

where k_{AC0}, k_{AC1}, and k_{AC2} are appropriate constant values. In order to model this engine fault, the constants k_{AC0}, k_{AC1}, and k_{AC2} are perturbed from their nominal values in the Simulink model. Reduction of air cooler effectiveness decreases the air cooler heat transfer coefficient, which should result in significant increase of engine scavenging receiver temperature and a

moderate rise of the exhaust gas temperature and turbocharger speed. The simulated air cooler effectiveness decrease was 30%.

< insert figure 6 >

As seen from the chart, the detection algorithm immediately detects the fault, as the control statistic rises above the UCL. The initial out-of-limits response is due to the transient phase of the engine simulator, since, for the fault detector to work, steady-state operation is assumed.

Furthermore in Table 5, details of the sensor values and 3σ individual limits are shown. As expected, engine scavenging receiver temperature (TO5) is significantly increased (being out of its 3σ limits), while exhaust gas temperature (TO4) and turbocharger speed (N_tc) are also increased but within their respective 95% limits. This behaviour demonstrates the effectiveness of the multivariable approach, since individual components may stay within their respective statistical confidence limits, while the sample as a whole is well out of its bounds.

< insert table 5 >

4. DSS software implementation

4.1. Generics

The DSS software implementation is based on the necessity to provide a software platform that would facilitate expandability properties combined with a user-friendly interface. For the former requirement, the software is designed in a generic manner, being able to address a large collection of setups, regardless of the different trip routes and ship or engine types, while for the latter requirement, a Graphical User Interface (GUI) is provided, requiring only problem-relevant inputs, thus without necessitating expert knowledge on multicriteria decision making or fault detection theory.

To this direction, a modular implementation has been followed for the DSS software, where the voyage plan development and the fault detection functionalities are developed as different modules, accompanied by separate GUIs. This allows the end users to select to deploy only the module necessary to address their needs, as well as to follow different execution patterns for each module (e.g. the voyage plan development can be invoked on demand, while the fault detection module can be executed in pre-defined time intervals, using a task scheduler).

4.2. Voyage plan development module implementation

The GUI for the voyage plan module is developed in MATLAB and includes the following structural components as separate graphical panels:

- Trip data;
- Ship data;
- User data and preferences.

The data related to the specific trip/route and the data related to the ship and engine type are the necessary input data for designing all the alternative voyage plans. The user preferences, such as criteria weights or constraints, are then utilised to determine voyage plans that are

infeasible (i.e. violating hard constraints), as well as to provide the basis on which the alternative voyage plans will be evaluated.

The execution of this DSS module starts with the provision of the trip data in the corresponding panel, as displayed in Figure 7. From this panel, the departure and arrival ports are selected from the available main routes database, where each main route is divided in segments, based on a list of coordinates. Subsequently, weather predictions in each segment of the main route are retrieved as a list of tuples containing information on the significant wave height, mean period and direction of waves. In addition, specific types of fuels can be selected for each route segment, addressing possible restrictions on fuel consistency enforced by international sailing regulations. Finally, the maximum width along the main route is defined, regulating the allowed deviation from the main course (channel width), which enables the generation of alternative trip routes under a pre-defined segmentation algorithm. In particular, for each segment of the main route, four alternative options within the channel are defined, one deviating to the starboard side of the ship, one deviating to the port side and two zig-zag options. An example of the alternative routes for a given channel width is shown in Figure 8a. Furthermore, in order to produce non symmetrical alternatives, a random factor can be activated on the algorithm (checking the option random perturbation in the dialog box of Figure 7) that produces irregular alternatives (deviations of the main course), as illustrated in the Figure 8b. The latter non-symmetrical perturbations permit us to better distinguish between alternatives near optimum results.

< insert figure 7 >

< insert figure 8 >

Of course, it is important to emphasise here that new main route (e.g. port pairs along with route coordinates), as well as new fuel types, can be defined and stored. The new elements will be available on the current planning task, as well as on future platform deployments.

Moving forward to the ship-related data panel shown in Figure 9, inputs related to the model and the condition of the ship are required. Here, the model of the ship is selected from a list of available models, as well as the load condition (full/ballast), the age of the ship and the time from the last hull cleaning. Moreover, the design speed (mean speed) along the main route, as well as its allowed deviation is defined.

< insert figure 9 >

This set of inputs, along with the route data, is utilised by the available model of the ship, in order to estimate the fuel consumption, ETA and emissions in each alternative voyage plan.

Finally, in the user preferences panel shown in Figure 10, the final inputs to the multicriteria decision algorithm are provided. Here, the cost of each fuel type is provided, along with upper bound constraints on the trip duration, the fuel consumption and the CO_2 and SO_2 emissions. In addition, the DM can indicate preference over some criteria (e.g. travel time over emissions), by adjusting the default criteria weights on the panel.

< insert figure 10 >

Once the user preference inputs are provided, the multicriteria analysis process initiates. Here, a table with all the alternative voyage plans is created and the model of the ship is utilised to

estimate the performance of each alternative plan over the defined criteria. When the multicriteria table is generated, an initial process rejects the voyage plans that violate the constraints, and the remaining plans are passed to PROMETHE II for ranking.

The final outcome of the multicriteria decision making process, i.e. the complete ranking of the alternative voyage plans is shown in Figure 11. Here, the performance – with respect to the defined criteria – of the first 10 in the ranking alternative voyage plans is shown, as well as the coordinates, speeds and fuel types per segment of the very first plan. Moreover, a map of the route implied by this first in the ranking voyage plan is included for visualisation purposes.

< insert figure 11 >

4.3. Fault Detection module implementation

The Fault Detection module is also implemented in MATLAB. Here, the pre-defined set of engine parameters measurements defined in Section 3.2 is retrieved, and the measurements are evaluated over the developed fault detection model of the engine. Subsequently, the response of the fault detection module ("healthy operation" or "engine fault") is produced. In addition, in order to assist the maintenance team to make informative decisions, the mean values of the trained model, as well as the indicative operation range for each parameter, are also provided (see Figure 12) along with the result of the fault detection process.

< insert figure 12 >

4.4. Data Acquisition

Both the voyage plan development and fault detection modules rely on available inputs from external sources; in the former case, a weather prediction service has to provide forecasts on the wave conditions along the main route, while in the latter case, engine performance parameters measurements have to be available. In order to develop a generic software solution, the ability to retrieve the required information from different sources (e.g. various weather services) or through different technologies (e.g. different ship SCADA systems) is essential.

In an effort to achieve this, a communication interface has been developed, facilitating a generic communication protocol. To start with, a data model for the exchange has been defined, containing all the necessary basic definitions (e.g. coordinates, route segments, wave information, etc.), as well as the required input data structures for the modules (table of wave information for the voyage plan and engine parameters measurements for the fault detection). Note here, that the responses of the modules are also defined, in case logging of the outcome of the DSS is required. Subsequently, a set of java classes defining the interface have been generated and exported to a java library file (jar file). Finally, the data exchange is achieved through calling specific RESTful web services (Richardson and Ruby, 2008) and exchanging object instances of the defined interface classes as JavaScript Object Notation (JSON) messages, as follows:

- Voyage plan module:

1. A request containing the main route coordinates is sent from the DSS and the response is a table containing the wave forecasts in each segment of the main route;
2. Upon completion, a message containing the data of the first in the ranking voyage plan, i.e. the route, along with the speeds and fuel types in each segment is communicated.

- Fault Detection module:
    1. An empty request is sent from the DSS and the response is a vector containing the pre-defined collection of engine parameters measurements;
    2. Upon completion, a message containing the engine status, as indicated by the fault detection process, is communicated.

This way, the data-exchange mechanism is defined without posing any constraints on the types of data sources or hardware and software infrastructure of the server, thus any external tool can provide the required data to the DSS.

5. Concluding remarks

Making cost effective and environmental friendly voyage and maintenance planning decisions are processes difficult to handle manually due to the numerous factors (weather conditions, speeds, load conditions, engine states, etc.) that affect ship performance and need to be considered. To this end, a DSS is proposed herein, that supports the development of cost effective and environmental friendly voyage plans, and the diagnosis of engine failures in order to timely develop maintenance plans.

For its first purpose i.e. the development of voyage plans, fed with several data concerning the involved ports, the main route connecting them, the prevailing sea states, currents and winds, around this route, as well as the particular ship that will undertake the trip and its load condition, a range of acceptable mean speeds as well as any existing constraints on fuel consumption, emitted pollutants and arrival time, the DSS develops and presents to the user several alternative voyage plans ranked via PROMETHE according to the preferences that he/she has expressed to criteria such as fuel consumption, pollutant emissions and travel time.

For its second purpose, i.e. the fault diagnosis, a multivariable control chart based on the Mahalanobis distance is used to take into account the interrelation of the various measured variables. Extensive simulations of normal engine operation provided the no-fault statistics, while selective fault conditions were used to verify the effectiveness of the employed algorithm.

The software implementation of the DSS has been based in MATLAB adopting a modular architecture whereby different independent software modules implement the two DSS constituent modules so that they can be deployed both or individually according to the needs of the user. In addition, in an effort to provide a generic software solution, the required input data are retrieved from dedicated web-services, following specific communication and data exchange protocols.

In this first version of the DSS, both the voyage plan development and the fault diagnosis modules have been developed based on a specific ship and engine type. It is however, possible to extend the DSS so as to consider additional ship and engine types by developing corresponding ship and engine models and structures. Another area for future research and

development concerns the way that the voyage plan development problem has been addressed in this DSS version. The particular problem is a stochastic one since the evaluations of the considered alternatives, and thus the resulting ranking, depend upon parameters such as the sea states, currents and winds, which are stochastic in nature. The approach followed herein, however, considers the problem as deterministic and does not take into account the uncertainty involved in the weather predictions. An additional and interesting therefore future extension would be to consider the voyage plan development problem in its real stochastic dimensions and examine the use of alternative MCDA approaches (Stewart, 2005), more suitable for decision making under uncertainty conditions.

Acknowledgements

This research is implemented through the Operational Program "Competitiveness and Entrepreneurship" (OPCE II) of the National Strategic Reference Framework (NSRF) 2007-2013 of the Greek Ministry of Development and Competitiveness and is co-financed by the European Union (European Regional Development Fund) and Greek National Funds. The contents of the paper reflect the views of the authors, who are responsible for the accuracy of the data presented herein.

References

Banisoleiman, K. and Rattenbury, N. (2006). 'Reliability trends, operating issues and acceptance criteria related to exhaust gas turbochargers used in the marine industry - a classification society view' in *Institution of Mechanical Engineers: 8th International Conference on Turbochargers and Turbocharging*, CRC Press, pp. 289-304.

Benvenuto, G. and Campora, U. (2007). *Performance prediction of a faulty marine diesel engine under different governor settings*. http://www.icmrt07.unina.it/Proceedings/Papers/c/22.pdf (Accessed 30 April 2013).

Bersimis, S., Panaretos, J. and Psarakis, S. (2005). Multivariate statistical process control charts and the problem of interpretation: A short overview and some applications in industry, *MPRA Paper No. 6397*, http://mpra.ub.uni-muenchen.de/6397/ (Accessed 1 January 2014).

Brans, J.-P. and Mareschal, B. (2005). 'PROMETHEE methods', in Figueira, J., Greco, S. and Ehrgott, M. (Eds.), *Multiple Criteria Decision Analysis: State of the Art Surveys*, Springer, pp. 163-195.

Cebi, S., Celik, M., Kahraman, C. and Deha Er, I. (2009). 'An expert system towards solving ship auxiliary machinery troubleshooting: SHIPAMT SOLVER', *Expert Systems with Applications*, Vol. 36, pp. 7219-7227.

EC (2011). *Staying ahead of the wave: Towards greener, safer, and more competitive waterborne transportation*. Studies and Reports, European Commission, Directorate-General for Research and Innovation, Directorate H – Transport, Unit H.2 - Surface transports, European Union, Brussels, Belgium.

Figueira, J., Greco, S. and Ehrgott, M. (Eds) (2005). *Multiple Criteria Decision Analysis: State of the Art Surveys*, Springer.

Heywood, J.B. (1988). '*Internal Combustion Engines Fundamentals*', McGraw-Hill.

Hountalas, D.T. (2000). 'Prediction of marine diesel engine performance under fault conditions', *Applied Thermal Engineering*, Vol. 20, pp. 1753-1783.

Kawasaki, Y. (1980). 'The marine diesel engine and its reliability problems', *Bulletin of the Marine Engineers Society of Japan*, Vol. 8, pp. 3-13.

Kosmas, O.T. and Vlachos, D.S. (2012). 'Simulated annealing for optimal ship routing', *Computers & Operations Research*, Vol. 39, pp. 576-581.

Kyrtatos, N.P. (1989). 'A microcomputer based diesel engine simulator for advanced ship propulsion monitoring and control systems', *Naval Engineers Journal*, Jan 1989, pp. 66-72.

Lamaris, V.T. and Hountalas, D.T. (2010). 'A general purpose diagnostic technique for marine diesel engines – Application on the main propulsion and auxiliary diesel units of a marine vessel', *Energy Conversion and Management*, Vol.51 No. 4, pp. 740-753.

Lin, Y.H., Fang, M.-C. and Yeung R.W. (2013). 'The optimization of ship weather-routing algorithm based on the composite influence of multi-dynamic elements', *Applied Ocean Research*, Vol. 43, pp. 184-194.

Mason, R.L. and Young, J.C. (2002). *Multivariate Statistical Process Control with Industrial Applications*, ASA-SIAM.

Meier, E. (1981). 'A simple method of calculation and matching turbochargers', *Publication CH-T 120 163E*, Brown Boveri & Company Ltd, Baden, Switzerland.

Moffett, A. and Sarkar, S. (2006). 'Incorporating multiple criteria into the design of conservation area networks: a minireview with recommendations', *Diversity and Distributions*, (Diversity Distrib.), Vol. 12, pp. 125-137.

Psaraftis, H.N. and Kontovas, C.A. (2012). 'Speed models for energy-efficient maritime transportation: A taxonomy and survey', *Transportation Research Part C*, Vol. 26, pp. 331-351.

Richardson, L. and Ruby, S. (2008). *RESTful web services*. O'Reilly.

Rohsenow, W.M., Hartnett, J.P. and Ganic, E. (1985). *Handbook of Heat Transfer Fundamentals*, 2nd ed. McGraw-Hill.

San Cristóbal Mateo, J. R. (2012). *Multi-Criteria Analysis in the Renewable Energy Industry*, Springer.

Stewart, T.J. (2005). 'Dealing with uncertainties in MCDA', in Figueira, J., Greco, S. and Ehrgott, M. (Eds.), *Multiple Criteria Decision Analysis: State of the Art Surveys*, Springer, pp. 445-470.

Theotokatos, G. (2010). 'On the cycle mean value modelling of a large two-stroke marine diesel engine', *Proceedings of the Institution of Mechanical Engineers, Part M: Journal of Engineering for the Maritime Environment*, Vol. 224 No. 3, pp. 193-205.

Watson, N. and Janota, M.S. (1982). *Turbocharging the Internal Combustion Engine*, Macmillan.

Table 1. List of symbols adopted by the simulation model

Notation	
A	area (m^2)
BMEP	brake mean effective pressure (bar)
BSFC	Brake specific fuel consumption (g/kW h)
c_V	specific heat at constant volume (J/kg K)
h	specific enthalpy (J/kg)
H_L	fuel power heating value (J/kg)
I	polar moment of inertia (kg m^2)
k	coefficients
m	mass (kg)
$\dot{m}$	mass flow rate (kg/s)
MCR	maximum continuous rating
MVEM	mean value engine modelling
N	rotational speed (r/min)
p	pressure (Pa)
pr	pressure ratio
Q	torque (N m)
$\dot{Q}$	heat transfer rate (W)
R	gas constant (J/kg K)
t	time (s)
T	temperature (K)
u	specific internal energy (J/kg)
γ	ratio of specific heats
ζ	proportion of the chemical energy of the fuel contained in the exhaust gas
η	efficiency
Subscripts	
a	air
amb	ambient
AC	air cooler
AF	air filter
BL	blower
$comb$	combustion
cyl	cylinder
C	compressor
d	downstream
ep	exhaust pipe
ew	entrained water
E	engine
ER	exhaust receiver
f	fuel
i	isentropic
in	inlet
out	outlet
P	propeller
SC	scavenging receiver
Sh	shafting system
T	turbine
TC	turbocharger
u	upstream

Table 2. Simulated engine faults

Fault no.	Fault description
0	healthy operation – no fault
1	dirty air filter
2	air cooler fouling
3	air cooler pressure drop increase
4	compressor fouling
5	turbine fouling
6	exhaust piping system fouling
7	variation of cylinder flow area (blockage/worn scavenging ports/exhaust valve)
8	cylinder components fault

Table 3. Fault cause-effect table

	Parameters	Air filter blockage	Air cooler fouling	Air cooler pressure drop	Compressor fouling	Turbine fouling	Exhaust piping system fouling	Cylinder flow area variation	Cylinder components fault
1	Propeller resistance (disturbance input – non measurable)								
2	Ambient water temperature (K) (disturbance input-measurable)								
3	Air cooler cooling water inlet temperature (K) (disturbance input – measurable)								
4	Rack position (control input)								
5	Engine speed (rpm) (system output)								
6	Turbocharger speed (rpm)				X	X			
7	Engine brake power (kW)								
8	Scavenging air receiver pressure (Pa)				X	X			X
9	Exhaust gas receiver pressure (Pa)				X	X			X
10	Gas temperature at turbine inlet (K)				X	X			X
11	Gas temperature at turbine outlet (K)				X	X			X
12	Compressor air MFR (kg/s)				X	X			X
13	Air temperature at A/C inlet (compressor exit) (K)							X	X
14	Air temperature at A/C outlet (K)		X		X				
15	Air cooler pressure drop (air side) (Pa)			X					
16	Air filter pressure drop (Pa)	X					X		

Table 4. Input variable intervals

	Variable	Interval
1	Propeller law constant	0.125 × (0.7 to 1) 6 values
2	Air cooler cooling water inlet temperature (°C), *Twac*	25-35 °C 11 values
3	Ambient air temperature (°C), *Ta*	11-46°C 11 values
4	Rack position, *FR*	0.6-1 11 values

Table 5. Engine parameters values for air cooler fouling fault

	0	1	2	3	4	5	6	7
	Kq	**Twac °C**	**Ta °C**	**FR**	**Neng rpm**	**N_tc rpm**	**Pbeng MW**	**p_sc bar**
M	0.106	28.85	27.35	0.8	1.511	151.31	8.46	2.83
Σ					0.16	20.79	2.19	0.6
$\mu+3\sigma$	0.0875	25	10	0.6	1.991	213.68	15.03	4.63
$\mu-3\sigma$	0.125	35	45	1	1.03	88.94	1.89	1.03
fault	0.093	33	27.99	0.9829	1.8	192	12.37	4.06
	8	9	10	11	12	13	14	15
	p_er bar	**T_er °C**	**TO4 °C**	**mfr_c kg/s**	**TO2 °C**	**T_sc °C**	**DPac Pa**	**Dpfilt Pa**
M	2.65	399.67	281.58	24.48	155.37	51.87	1180	90
Σ	0.56	29.5	23.89	5.13	31.2	7.7	311	37
$\mu+3\sigma$	4.33	488.17	353.25	39.87	248.97	74.97	2113	200
$\mu-3\sigma$	0.97	311.17	209.91	9.09	61.77	28.77	244	6
fault	3.79	486.9	313.4	33.11	217.9	102.4	1702	162

Kq: propeller law constant
Twac: Air cooler cooling water inlet temperature
Ta: Ambient air temperature
FR: fuel rack position
Neng: engine rotational speed
N_tc: turbocharger rotational speed
Pbeng: engine brake power
p_sc: scavenging receiver pressure
p_er: exhaust receiver pressure
T_er: exhaust receiver temperature
TO4: temperature of exhaust gas exiting engine
mfr_c: engine air mass flow rate
TO2: temperature of air exiting compressor
T_sc: scavenging receiver temperature
DPac: air cooler pressure drop
DPfilt: air filter pressure drop

Figure captions

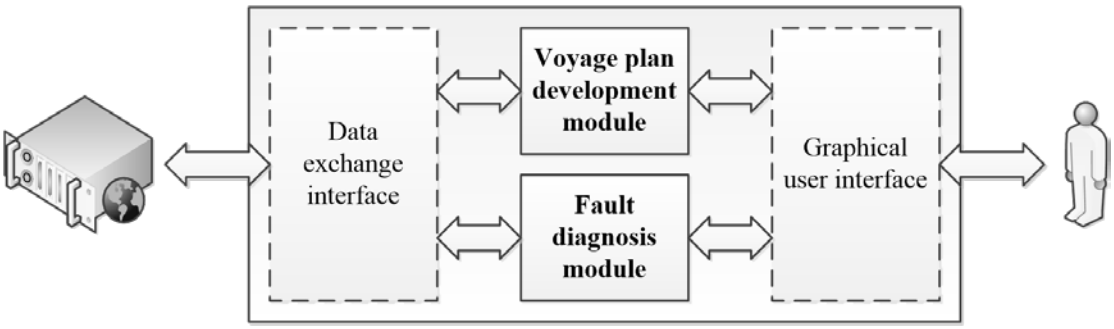
Data exchange interface
Voyage plan development module
Fault diagnosis module
Graphical user interface

Figure 1

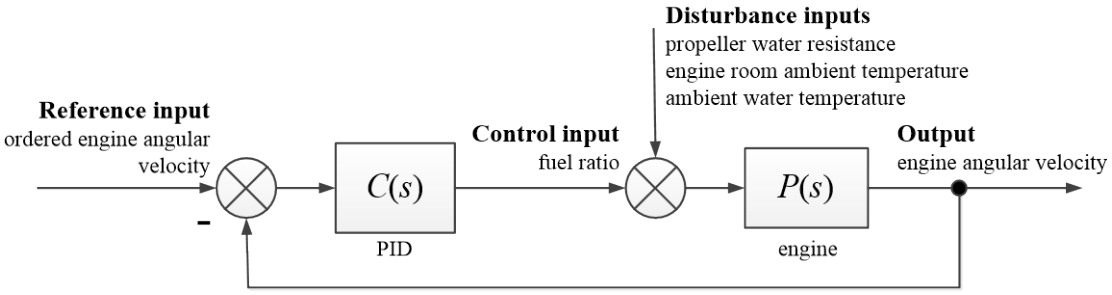
Disturbance inputs
propeller water resistance
engine room ambient temperature
ambient water temperature
Reference input
ordered engine angular velocity
Control input
fuel ratio
Output
engine angular velocity
C(s)
PID
P(s)
engine
-

Figure 2

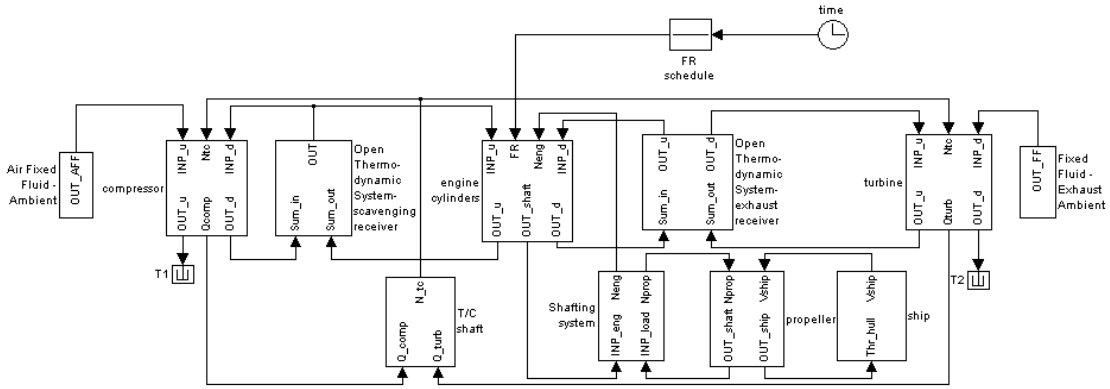
time
FR
schedule
Air Fixed
Fluid -
Ambient
OUT_AFF
compressor
INP_u
Ntc
INP_d
OUT_u
Qcomp
OUT_d
OUT
Sum_in
Sum_out
Open
Thermo-
dynamic
System-
scavenging
receiver
engine
cylinders
INP_u
FR
Neng
INP_d
OUT_u
OUT_shaft
OUT_d
OUT_u
OUT_d
Sum_in
Sum_out
Open
Thermo-
dynamic
System-
exhaust
receiver
turbine
INP_u
Ntc
INP_d
OUT_u
Qturb
OUT_d
OUT_FF
Fixed
Fluid -
Exhaust
Ambient
T1
T2
N_tc
Q_comp
Q_turb
T/C
shaft
Shafting
system
Neng
INP_eng
Nprop
INP_load
OUT_shaft
Nprop
Vship
OUT_ship
propeller
Vship
Thr_hull
ship

Figure 3

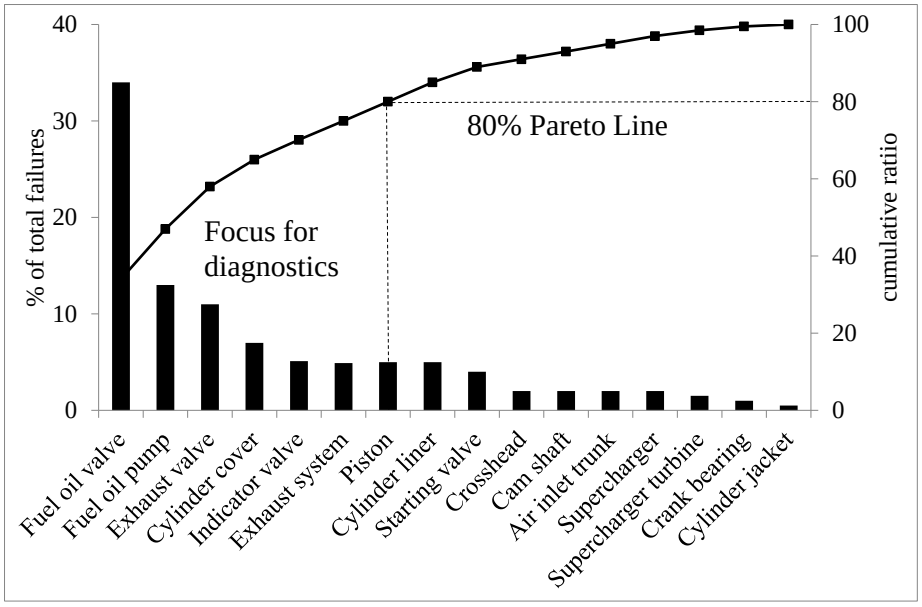
40
30
20
10
0
% of total failures
100
80
60
40
20
0
cumulative ratiio
80% Pareto Line
Focus for
diagnostics
Fuel oil valve
Fuel oil pump
Exhaust valve
Cylinder cover
Indicator valve
Exhaust system
Piston
Cylinder liner
Starting valve
Crosshead
Cam shaft
Air inlet trunk
Supercharger
Supercharger turbine
Crank bearing
Cylinder jacket

Figure 4

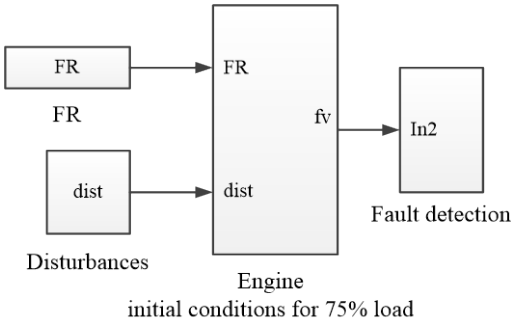
FR
FR
dist
Disturbances
FR
dist
fv
Engine
initial conditions for 75% load
In2
Fault detection

Figure 5

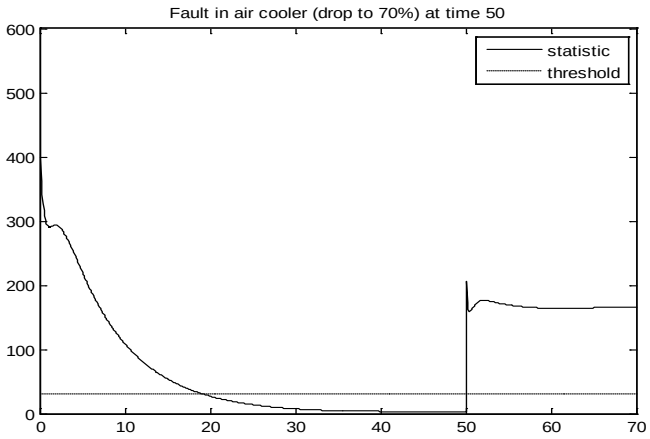
Fault in air cooler (drop to 70%) at time 50
statistic
threshold
600
500
400
300
200
100
0
0
10
20
30
40
50
60
70

Figure 6

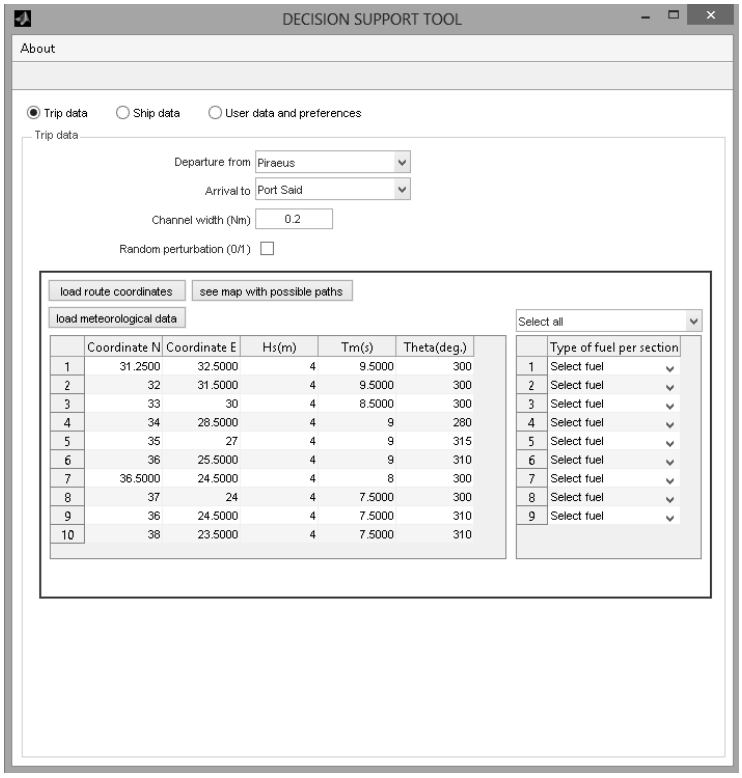
DECISION SUPPORT TOOL
About
Trip data
Ship data
User data and preferences
Trip data
Departure from
Piraeus
Arrival to
Port Said
Channel width (Nm)
0.2
Random perturbation (0/1)
load route coordinates
see map with possible paths
load meteorological data
Select all
Coordinate N
Coordinate E
Hs(m)
Tm(s)
Theta(deg.)
1 31.2500 32.5000 4 9.5000 300
2 32 31.5000 4 9.5000 300
3 33 30 4 8.5000 300
4 34 28.5000 4 9 280
5 35 27 4 9 315
6 36 25.5000 4 9 310
7 36.5000 24.5000 4 8 300
8 37 24 4 7.5000 300
9 36 24.5000 4 7.5000 310
10 38 23.5000 4 7.5000 310
Type of fuel per section
1 Select fuel
2 Select fuel
3 Select fuel
4 Select fuel
5 Select fuel
6 Select fuel
7 Select fuel
8 Select fuel
9 Select fuel

Figure 7

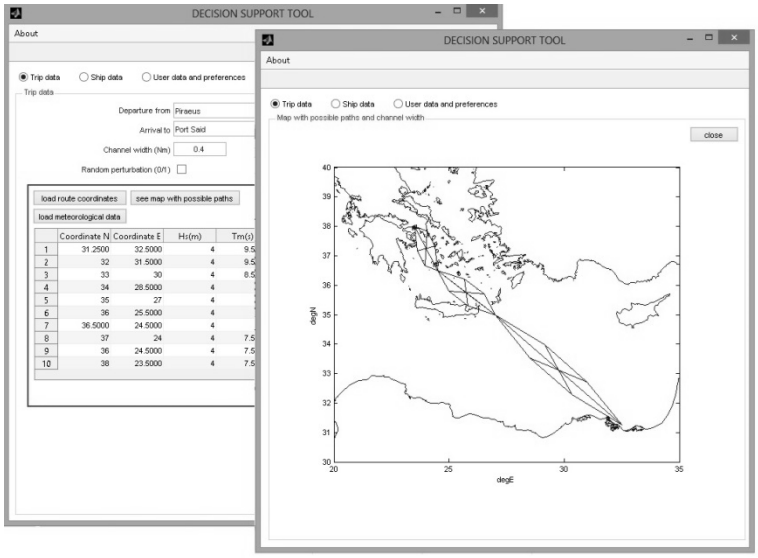
DECISION SUPPORT TOOL
About
Trip data
Ship data
User data and preferences
Departure from
Piraeus
Arrival to
Port Said
Channel width (Nm)
0.4
Random perturbation (0/1)
load route coordinates
see map with possible paths
load meteorological data
Map with possible paths and channel width
close
degN
degE

(a)

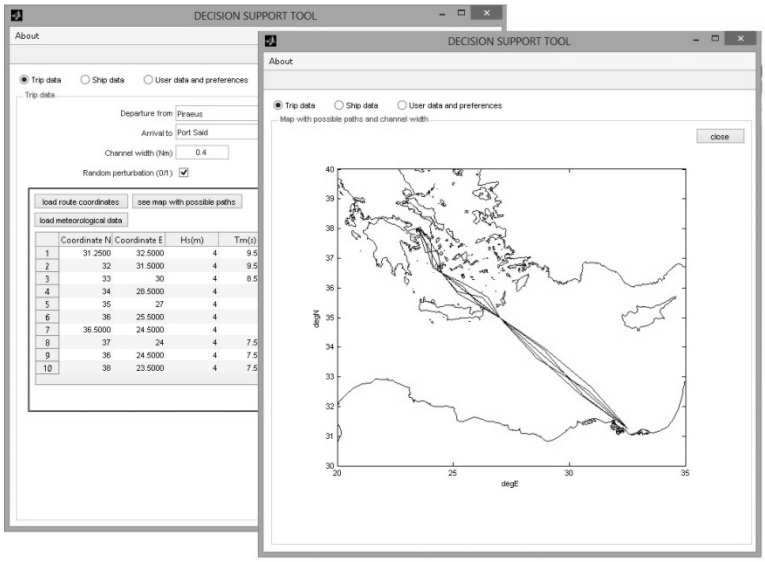
DECISION SUPPORT TOOL
About
Trip data
Ship data
User data and preferences
Departure from
Piraeus
Arrival to
Port Said
Channel width (Nm)
0.4
Random perturbation (0/1)
load route coordinates
see map with possible paths
load meteorological data
Map with possible paths and channel width
close
degN
degE

(b)

Figure 8

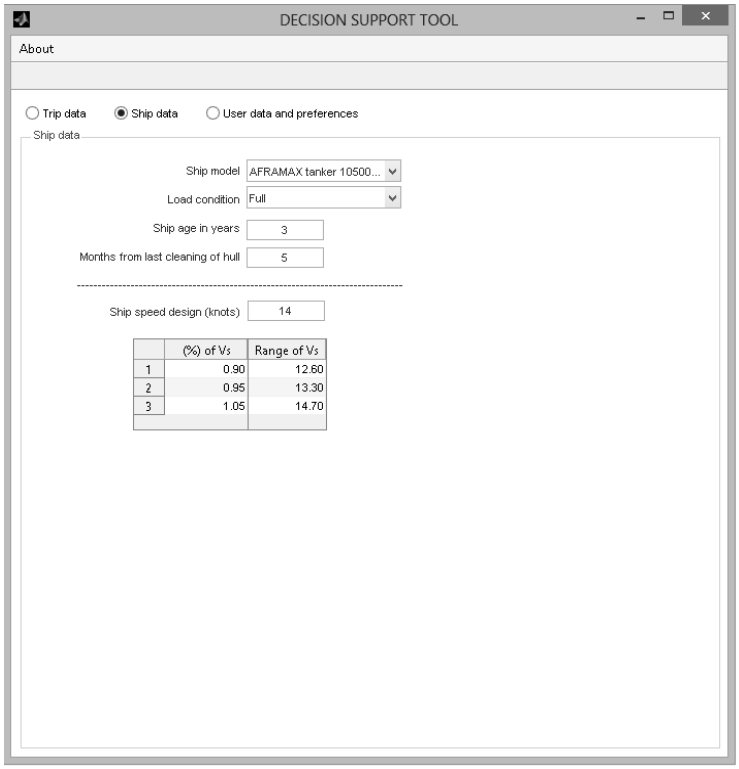
DECISION SUPPORT TOOL
About
Trip data
Ship data
User data and preferences
Ship data
Ship model
AFRAMAX tanker 10500...
Load condition
Full
Ship age in years
3
Months from last cleaning of hull
5
Ship speed design (knots)
14
(%) of Vs
Range of Vs
1
0.90
12.60
2
0.95
13.30
3
1.05
14.70

Figure 9

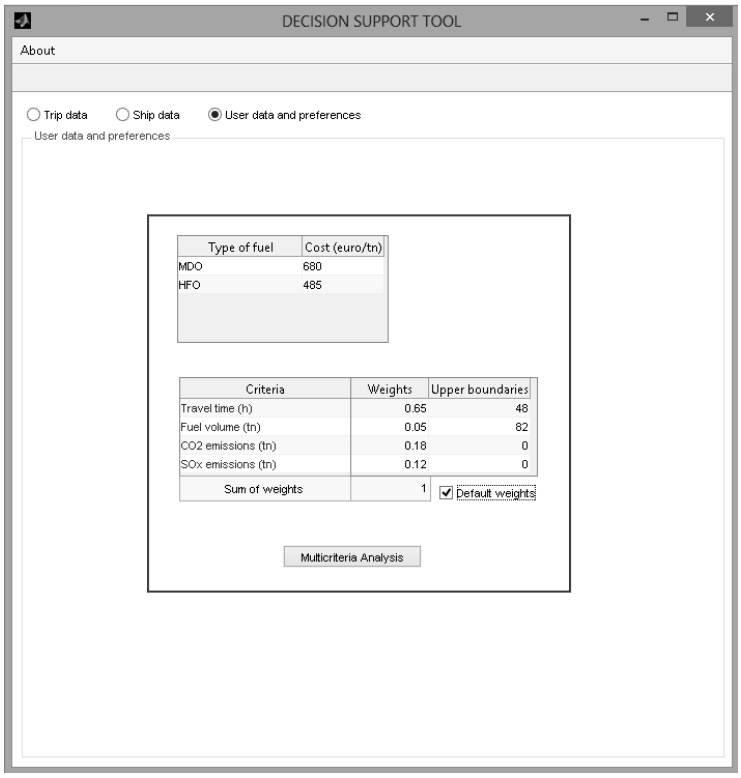
DECISION SUPPORT TOOL
About
Trip data
Ship data
User data and preferences
User data and preferences
Type of fuel
Cost (euro/tn)
MDO
680
HFO
485
Criteria
Weights
Upper boundaries
Travel time (h)
0.65
48
Fuel volume (tn)
0.05
82
CO2 emissions (tn)
0.18
0
SOx emissions (tn)
0.12
0
Sum of weights
1
Default weights
Multicriteria Analysis

Figure 10

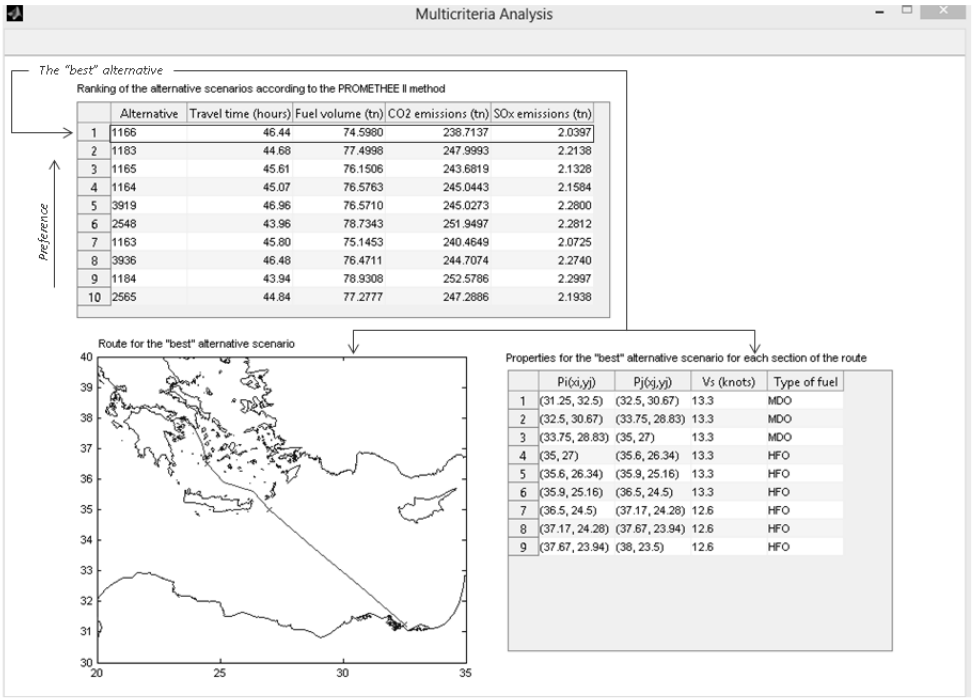
Multicriteria Analysis
The "best" alternative
Ranking of the alternative scenarios according to the PROMETHEE II method
Preference
Alternative | Travel time (hours) | Fuel volume (tn) | CO2 emissions (tn) | SOx emissions (tn)
1 1166 46.44 74.5980 238.7137 2.0397
2 1183 44.68 77.4998 247.9993 2.2138
3 1165 45.61 76.1506 243.6819 2.1328
4 1164 45.07 76.5763 245.0443 2.1584
5 3919 46.96 76.5710 245.0273 2.2800
6 2548 43.96 78.7343 251.9497 2.2812
7 1163 45.80 75.1453 240.4649 2.0725
8 3936 46.48 76.4711 244.7074 2.2740
9 1184 43.94 78.9308 252.5786 2.2997
10 2565 44.84 77.2777 247.2886 2.1938
Route for the "best" alternative scenario
40
39
38
37
36
35
34
33
32
31
30
20
25
30
35
Properties for the "best" alternative scenario for each section of the route
Pi(xi,yi) | Pj(xj,yj) | Vs (knots) | Type of fuel
1 (31.25, 32.5) (32.5, 30.67) 13.3 MDO
2 (32.5, 30.67) (33.75, 28.83) 13.3 MDO
3 (33.75, 28.83) (35, 27) 13.3 MDO
4 (35, 27) (35.6, 26.34) 13.3 HFO
5 (35.6, 26.34) (35.9, 25.16) 13.3 HFO
6 (35.9, 25.16) (36.5, 24.5) 13.3 HFO
7 (36.5, 24.5) (37.17, 24.28) 12.6 HFO
8 (37.17, 24.28) (37.67, 23.94) 12.6 HFO
9 (37.67, 23.94) (38, 23.5) 12.6 HFO

Figure 11

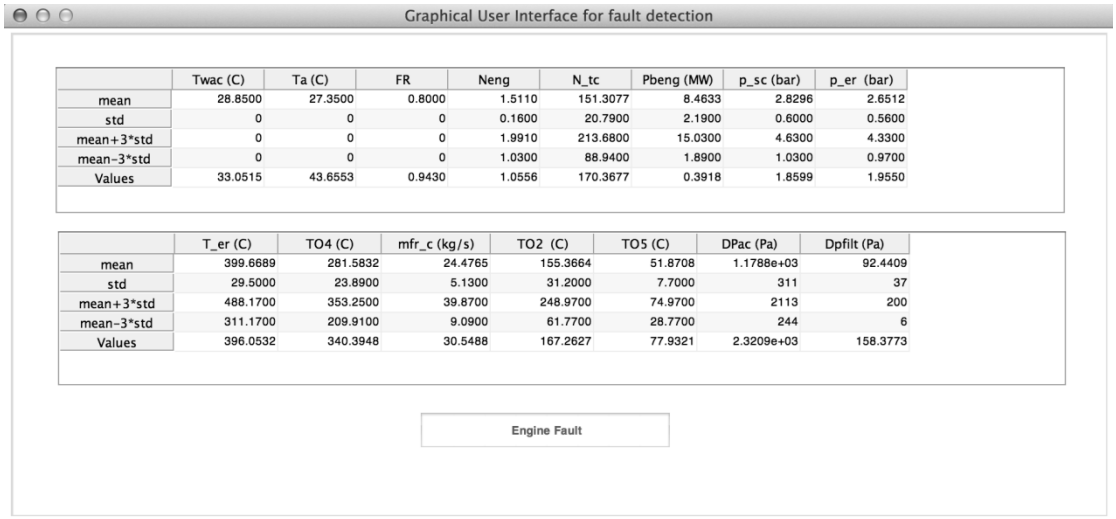

	Twac (C)	Ta (C)	FR	Neng	N_tc	Pbeng (MW)	p_sc (bar)	p_er (bar)
mean	28.8500	27.3500	0.8000	1.5110	151.3077	8.4633	2.8296	2.6512
std	0	0	0	0.1600	20.7900	2.1900	0.6000	0.5600
mean+3*std	0	0	0	1.9910	213.6800	15.0300	4.6300	4.3300
mean-3*std	0	0	0	1.0300	88.9400	1.8900	1.0300	0.9700
Values	33.0515	43.6553	0.9430	1.0556	170.3677	0.3918	1.8599	1.9550

	T_er (C)	TO4 (C)	mfr_c (kg/s)	TO2 (C)	TO5 (C)	DPac (Pa)	Dpfilt (Pa)
mean	399.6689	281.5832	24.4765	155.3664	51.8708	1.1788e+03	92.4409
std	29.5000	23.8900	5.1300	31.2000	7.7000	311	37
mean+3*std	488.1700	353.2500	39.8700	248.9700	74.9700	2113	200
mean-3*std	311.1700	209.9100	9.0900	61.7700	28.7700	244	6
Values	396.0532	340.3948	30.5488	167.2627	77.9321	2.3209e+03	158.3773

Figure 12